

Received December 6, 2017, accepted January 3, 2018, date of publication January 8, 2018, date of current version March 9, 2018.

Digital Object Identifier 10.1109/ACCESS.2018.2790433

# Perceptual Enhancement of Low Light Images Based on Two-Step Noise Suppression

HAONAN SU AND CHEOLKON JUNG<sup>ID</sup>, (Member, IEEE)

School of Electronic Engineering, Xidian University, X'ian, Shaanxi 710071, China

Corresponding author: Cheolkon Jung (zhengzk@xidian.edu.cn)

This work was supported in part by the National Natural Science Foundation of China under Grant 61271298 and in part by the International S&T Cooperation Program of China under Grant 2014DFG12780.

**ABSTRACT** Low-light images are seriously corrupted by noise due to the low signal-to-noise ratio. In low intensity, just-noticeable-difference (JND) is high, and thus the noise is not perceived well by human eyes. However, after contrast enhancement, the noise becomes obvious and severe, because JND decreases as intensity increases. Thus, contrast enhancement without considering human visual perception causes serious noise amplification in low-light images. In this paper, we propose perceptual enhancement of low-light images based on two-step noise suppression. We adopt two-step noise suppression based on noise characteristics corresponding to human visual perception. First, we perform noise aware contrast enhancement using a noise-level function. However, the increase of the intensity caused by contrast enhancement reduces JND in low intensity, which makes noise much more visible by human eyes. Second, we perceptually reduce noise in images while preserving details using a JND model, which represents noise visibility in contrast enhancement. We estimate the noise visibility based on the intensity change using luminance adaptation. Also, we extract image details by contrast masking and visual regularity, because textural regions have higher visibility thresholds than the smooth ones. Based on the human visual characteristics, we perform perceptual noise suppression using the JND model. Experimental results show that the proposed method perceptually enhances contrast in low-light images while successfully minimizing distortions and preserving details.

**INDEX TERMS** Contrast enhancement, just-noticeable-difference, low light, noise level function, noise reduction, human visual perception.

## I. INTRODUCTION

Low light images captured by digital cameras in low light condition have poor image quality with a narrow dynamic range and are seriously degraded by noise. The limited dynamic range distorts image contrast, which results in the loss of informative textures. It affects the performance of many computer vision applications such as object detection, recognition, and tracking. Thus, it is required to perform low light image enhancement considering both contrast enhancement and noise reduction.

## A. RELATED WORK

Many attempts have been made to enhance the contrast of low light images. They are mainly classified into three groups: 1) Non-linear mapping-based approaches such as gamma function, logarithm function, and power law functions, which are used as a preprocessing step of low light image enhancement [2], [3]; 2) Histogram-based schemes such as histogram

equalization (HE), contrast limited adaptive histogram equalization (CLAHE) [4], contrast enhancement by histogram modification framework (HMF) [5], optimal contrast-tone mapping (OCTM) [6], adaptive gamma correction with weighting distribution(AGCWD) [7], and adaptive extended piecewise histogram equalisation (AEPHE) [8]; 3) Multiscale analysis-based methods which decompose an image into several subbands and enhance frequency components in each subband [9]–[11]. Histogram-based approaches separate gray levels of higher probability further to obtain pixel mapping curves for histogram modification. They increase the difference between two altered gray levels and preserve the relative order of them, which makes histogram-based approaches not suffer from ringing artifacts [6]. Thus, they have much attention by researchers. However, they are not effective in considering noise characteristics and image locality, thus leading to noise amplification after contrast enhancement. This is because low light images contain serious noise in large

flat regions with dark intensity. Histogram-based approaches cause noise amplification while enhancing these regions. Therefore, the noise reduction has been applied to the contrast enhancement in recent years [12]–[14].

Some researchers have performed low light image enhancement based on the observation that the inverted low light images are similar to hazy images [15]–[18]. Thus, they applied haze removal to enhance low light images [15]. Li *et al.* [16] and Zhang *et al.* [17] adopted a dark channel prior to enhance images. However, the former one applied superpixel-based adaptive denoising to improve denoising performance while the latter one introduced joint bilateral filtering to the original green component as the edge image to suppress noise. Shi *et al.* [18] utilized group-based sparse representation to accurately estimate transmittance of the inverted input image based on intrinsic local sparsity and nonlocal self-similarity. However, the dark channel prior-based contrast enhancement produced serious visible noise due to the strong luminance enhancement, and also led to the color cast problem, i.e. hue shift to unwanted colors such as red and green.

Other researchers have conducted noise removal in the transform domain such as DCT and wavelet [19]–[21]. They reduced noise in the high frequency layer while stretching dynamic range in the low frequency layer. Łoza *et al.* [19] designed non-linear luminance enhancement with noise reduction based on local dispersion of wavelet coefficients and shrinkage function. Sun and Jung [20] performed contrast enhancement with noise reduction in the wavelet domain. The contrast enhancement was performed by CLAHE in the low-pass subband, while the noise reduction was conducted by a nonlinear transform in the high-pass subbands. Jung *et al.* [21] also achieved contrast enhancement in the wavelet domain but performed noise reduction based on content-based total variation (TV) diffusion considering noise and edges in the high-pass subbands. However, they amplified noise in low light images after contrast enhancement without considering noise characteristics.

In addition, more works on low light image enhancement has been studied as follows [22]–[27]. Rivera *et al.* [22] acquired the 256 transformation function by content-aware HE which considered edge-contrast pairs. Edge-contrast pairs had the intensity difference between neighboring pixels larger than a threshold. They enhanced images by fusing the mapping curves which simulated the human visual system (HVS). However, this method could not provide insufficient enhancement in contrast and luminance for low light images. Lim *et al.* [23] first performed contrast enhancement on noise-free pixels, and then interpolated the missed noisy pixels by low rank matrix completion. However, this method led to severe degradation of texture and details due to the removal of noise pixels. Liu *et al.* [24] combined denoising with contrast enhancement into a unified framework. They estimated a robust graph-based enhancement operator to enhance the contrast without noise amplification via a graph-signal smoothness prior. They performed denoising by sparse

coding formulation. Chouhan *et al.* [25] and Jha *et al.* [26] performed adaptive stochastic resonance-based enhancement in terms of perceptual quality in color and contrast, respectively. The former one did it in the spatial domain while the latter one performed in the DCT domain. Sugimura *et al.* [27] enhanced low light images by fusing RGB color images and near-infrared images under different exposure times.

For video enhancement, researchers have utilized spatiotemporal filters to remove inter- and intra-frame noise, and then performed tone mapping to enhance low light videos [2], [3], [28], [29]. Malm *et al.* [28] proposed structure-adaptive anisotropic filtering to reduce noise while preserving structure in videos. Then, they performed tone mapping by CLAHE [30]. Xu *et al.* [3] updated spatiotemporal filtering by considering motion in videos. They first performed spatial and temporal filtering independently, and then combined the filtering results based on the correlation between video motion and image anisotropy. They performed local contrast-based tone mapping to enhance low light videos. Kim *et al.* [29] first conducted motion adaptive temporal filtering before tone mapping, and then did NLM denoising after tone mapping. They performed tone mapping based on adaptive histogram adjustment using gamma correction with clipping thresholds.

Thus, most existing methods have performed contrast enhancement without considering noise characteristics and image locality, which causes serious noise amplification after contrast enhancement. Although some methods have noise reduction functions, the noise removal has seriously degraded textures and details in low light images without considering human visual perception and noise characteristics. Therefore, we introduce noise aware contrast enhancement to enhance low light images while preventing noise amplification. Moreover, we consider noise visibility in contrast enhancement to perceptually suppress noise while preserving details in images.

## B. CONTRIBUTIONS

In this paper, we propose low light image enhancement based on two-step noise suppression. To enhance low light images while successfully reducing noise and preserving details, we adopt noise level function (NLF) and just-noticeable-difference (JND) model in contrast enhancement. First, we convert RGB color space of the input image into YUV color space. Second, we perform noise aware contrast enhancement using a noise aware histogram to consider both local contrast and noise distribution. Noise aware contrast enhancement prevents contrast overstretching and noise amplification in large flat regions with dark intensity and severe noise. Third, we perform perceptual noise suppression in the detail layer based on the luminance adaptation and visual masking effect from the JND model. The JND-based noise suppression reduces noise while avoiding serious detail loss. Finally, we perform color enhancement to reproduce more natural-looking and vivid colors in images. Fig. 1 illustrates the entire block diagram of the proposed method.

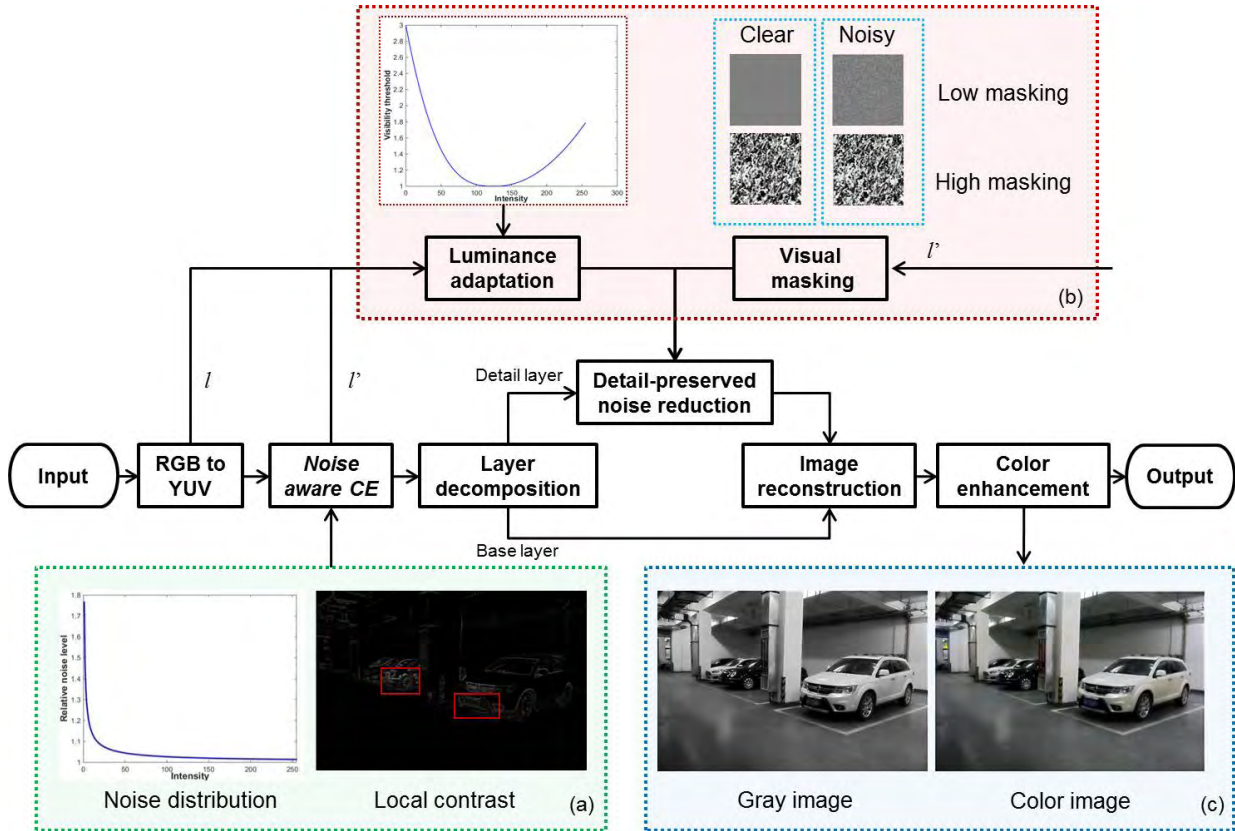


**FIGURE 1.** Entire block diagram of the proposed method.  $I$  and  $I'$  are intensities in the original image and its enhanced result, respectively. CE is contrast enhancement. (a) Noise distribution by Eq. (2) and local contrast by Eq. (3). (b) Luminance adaptation curve and visual masking effect (local region characteristics affect the noise visibility). Top: Smooth patch and its result with added noise. Bottom: Texture patch and its result with added noise. (c) Color enhancement.

Compared with existing methods, main contributions of this work are as follows:

- We use NLF and local contrast to acquire the noise aware histogram for contrast enhancement. The noise aware histogram successfully enhances the contrast of texture regions while preventing noise amplification in large dark regions with severe noise;
- We introduce a JND model based on luminance adaptation and visual masking into contrast enhancement to estimate noise visibility after contrast enhancement. Luminance adaptation measures the noise visibility caused by luminance enhancement, while visual masking measures the noise visibility on smooth and texture regions. The combination of two models achieves noise reduction while preserving details in enhanced results.
- Compared to our previous work [1], the proposed method employs luminance contrast and visual regularity to estimate visual masking effect, which leads to good detail preservation in contrast enhancement.

The remainder of this paper is organized as follows. In Section II, we explain the proposed method in detail, and experimental results are shown in Section III. Finally, conclusions are drawn in Section IV.

## II. PROPOSED METHOD

### A. NOISE AWARE CONTRAST ENHANCEMENT

We analyze noise amplification and over-enhancement that appear in low light images after contrast enhancement, and propose a noise aware histogram based on visual content and noise level. The noise aware histogram successfully attenuates noise amplification and over-enhancement in large flat regions with dark intensity.

a) Noise amplification by contrast enhancement: sensor noise in digital cameras is signal-dependent, which is represented by a generalized signal-dependent noise model [31], [32]. In this work, we use a generalized signal dependent noise model to represent sensor noise including poisson noise in low light images [32] [33]. Noise level function (NLF) for signal-dependent noise is expressed as follows [32]:

$$\sigma(I) = \sqrt{I^{2\gamma} \cdot \sigma_u^2 + \sigma_w^2} \quad (1)$$

where  $\gamma$  is the exponential parameter which controls the dependence on the signal;  $u$  and  $w$  are zero-mean Gaussian distributions with variances  $\sigma_u^2$  and  $\sigma_w^2$ , respectively. Based on  $\sigma(I)$ , we define the relative noise level (RNL)  $n(I)$  as

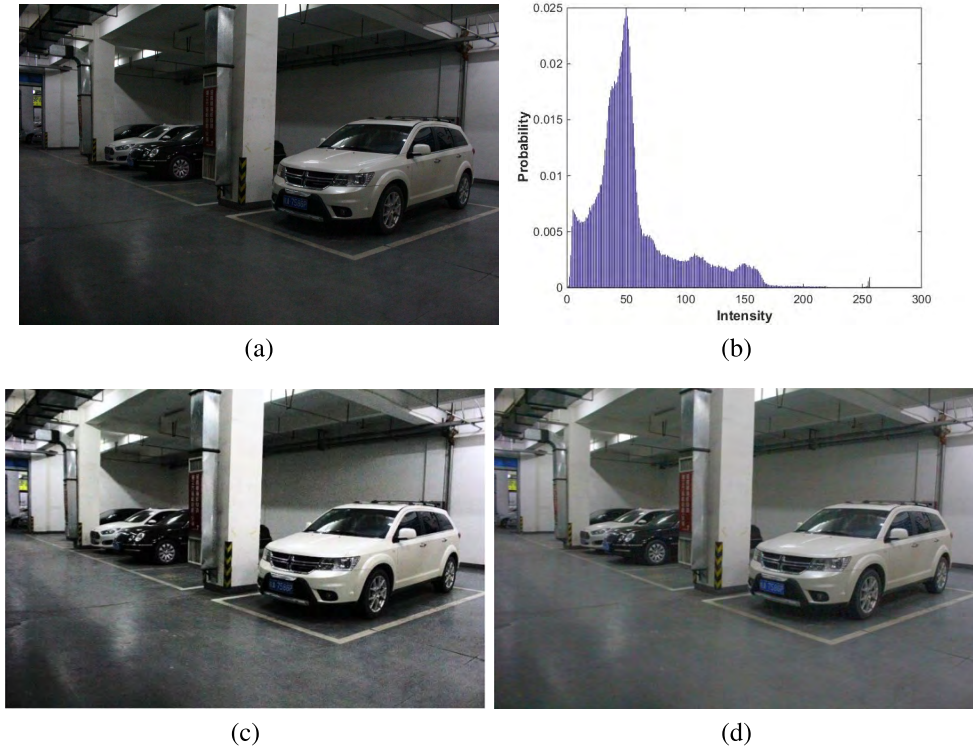


**FIGURE 2.** Enhanced results by AGCWD [7] and gamma function  $y = x^{0.5}$ . (a) Original image. (b) Histogram of (a). (c) Enhanced result by AGCWD [7]. (d) Enhanced result by gamma function.

follows:

$$n(I) = \frac{I + \sigma(I)}{I} \quad (2)$$

where  $I$  is the intensity obtained from noisy free pixels.  $\sigma(I)$  is the standard deviation of noise by NLF in (1); and  $n(I)$  represents the relative noise level to noise-free intensity. The left figure in Fig. 1(a) shows RNL varying with intensity which is defined as the ratio of noisy intensity to noise-free intensity. Larger RNL means higher effect of noise level on the intensity level. That is, RNL is big in dark intensity (0-15), and rapidly decreases varying as intensity increases. Thus, noise affects dark intensity more severely than the other intensities, and thus is serious in dark intensity. This is also validated in the right figure of Fig. 1(a) (see the red boxes). Therefore, low light images contain serious noise in dark intensity. Although serious noise appears in dark regions, low visual sensitivity in HVS to dark intensity reduces the noise visibility, thus making the noise invisible.

However, conventional contrast enhancement methods are not effective in considering the noise characteristics and image locality, which causes severe noise amplification and over-enhancement. There are two reasons of them: 1) Large flat regions with a narrow dynamic range makes high probability in the original histogram as shown in Fig. 2(b). High probability causes histogram over-stretching in these region after contrast enhancement, which results in over-enhancement of contrast and noise such as wall and

ground in Fig. 2(c). 2) Based on the noise characteristics (see the left figure in Fig. 1(a)), dark intensity should be enhanced little to prevent serious noise amplification. However, nonlinear mapping functions such as gamma correction and logarithmic mapping enhance dark intensity much more than the others, which cause much noise amplification in dark regions such as black car and plate number in Fig. 2(d). Therefore, we propose noise aware contrast enhancement to overcome these two problems considering noise characteristics and local contrast.

b) Noise aware histogram estimation: we estimate the noise aware histogram based on pixels with a larger local contrast than noise level to exclude serious noise pixels in large flat regions with dark intensity and prevent over-stretching these regions by contrast enhancement [34]. First, we estimate the local contrast  $c$  in a region as follows:

$$c(x, y) = \sqrt{\frac{(g_\sigma * l^2)(x, y)}{(g_\sigma * l)^2(x, y)}} \quad (3)$$

where  $l$  is a pixel in the original image; and  $g_\sigma$  is a Gaussian kernel with the standard deviation  $\sigma$ . Then, we obtain the histogram of high contrast pixels based on relative noise level (RNL) and local contrast as follows:

$$p(i) = \frac{\sum_{(x,y) \in B_i} l(x, y)}{\sum_{(x,y) \in S} l(x, y)} \quad (4)$$

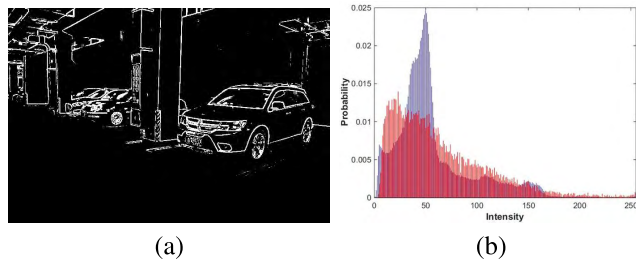


**FIGURE 3.** High contrast map in *Car* and its histograms. (a) High contrast map. (b) Original histogram (blue) for Fig. 2(a) and noise aware histogram (red) for (a).

where

$$S = \{(x, y) : c(x, y) > n(x, y)\} \quad (5)$$

$$B_i = \{(x, y) \in S : i = 0, 1, \dots, 255\} \quad (6)$$

where  $n(x, y)$  is estimated by (2), and  $I$  is calculated as  $I = g_\sigma * l$  for the approximation of noise free pixels.  $S$  is the set of high contrast pixels whose local contrast is higher than the noise level;  $B_i$  is the subset of  $S$  which contains the pixels whose intensity is  $i$ ; and  $n(x, y)$  is the relative noise level calculated by (2). Fig. 3(a) shows a high contrast map in *Car* by (5) where white pixels mean pixels with high contrast. The high contrast map is composed of high contrast pixels obtained by (5), which prevents noise pixels in flat regions from being contained in the noise aware histogram. Fig. 3(b) shows the noise aware histogram (red) obtained by (4)-(6) which removes most of noise pixels in dark regions while preventing histogram spikes which causes over-enhancement.

c) Contrast enhancement by noise aware histogram: we perform HE, OCTM [6], and AGCWD [7] for contrast enhancement from the noise aware histogram, and show the results in Fig. 4. As shown in the figure, HE avoids over enhancement in dark regions and large flat regions such as sofa and table in *Restaurant*. OCTM does not produce over enhancement in large flat regions by adding a constraint to each intensity increment. OCTM also prevents over enhancement in dark regions such as the black car in *Car*. AGCWD prevents over stretching in large flat regions such as wall and door in *Classroom*. That is, the noise aware histogram improves the contrast enhancement performance by successfully suppressing noise in dark and large flat regions. In this work, we adopt the noise aware OCTM [6] for low light image enhancement because OCTM [6] achieves contrast enhancement with the minimized tone distortion.

#### B. DETAIL-PRESERVED NOISE REDUCTION

With the increase of intensity by contrast enhancement, the visibility threshold of HVS decreases, and thus noise becomes obvious in human eyes. We estimate the visibility threshold using a JND model which represents the minimum intensity difference perceived by HVS, called luminance adaptation. Local textures also affect the visibility, called visual masking effect caused by interaction or interference

among visual stimuli. We estimate the visual masking effect based on the luminance contrast (gradient magnitude) and visual regularity (gradient regularity), and the noise visibility is larger in smooth regions than texture regions (see the right figure of Fig. 1(b)). Thus, the noise reduction should be larger in smooth regions than texture regions, which is beneficial to the detail preservation in images. We perform perceptual noise reduction based on a JND model to remove noise while preserving image details. We combine luminance adaptation (noise reduction) and visual masking (detail preservation) into a JND model.

Although noise aware contrast enhancement reduces noise in dark and large flat regions, noise still remains in the results as shown in Fig. 4. There are two main reasons: 1) Contrast enhancement brightens images but reduces JND threshold in low intensity (i.e. 15-127), which makes noise more visible (see left figure in Fig. 1(b)). 2) Global contrast enhancement performs coarse noise reduction without considering local characteristics in the spatial domain, but local characteristics (e.g. smooth and texture regions) have different visibility sensitivity to noise, called visual masking effect (see the right figure in Fig. 1(b)). Thus, we perform fine noise reduction based on a JND threshold (luminance adaptation) considering locality (visual masking). First, we conduct base-detail layer decomposition based on anisotropic diffusion-weighted bilateral filtering in Algorithm 1 [34] to extract the detail layer. Then, we perform noise reduction in the detail layer which contains much noise and details as shown in Fig. 5(c). Due to the first reason, we remove noise after the contrast enhancement using the variation of JND thresholds (luminance adaptation). Due to the second reason, we introduce two visual masking effects of contrast masking and regularity masking in the spatial JND model to represent luminance contrast and gradient regularity in local regions [35]. That is, we perform noise reduction differently according to the luminance contrast and visual regularity in a local region.

Then, we perform perceptual noise reduction in the detail layer using luminance adaptation factor  $LA(x, y)$  and visual masking factor  $VM(x, y)$  as follows:

$$d_{out}(x, y) = e \cdot VM(x, y) \cdot LA(x, y) \cdot d(x, y) \quad (7)$$

where  $d_{out}(x, y)$  and  $d(x, y)$  are outputs of noise reduction and noise aware contrast enhancement in the detail layer, respectively;  $e$  is the control parameter of noise reduction degree (we set  $e$  equals to 1 generally). We calculate  $LA(x, y)$  using the ratio of JND thresholds (luminance adaptation) before and after contrast enhancement as follows:

$$LA(x, y) = \frac{V(l'(x, y))}{V(l(x, y))} \quad (8)$$

where  $l(x, y)$  and  $l'(x, y)$  are the original image and its enhanced result by noise aware contrast enhancement, respectively; and  $V(x, y)$  is the visibility threshold generated by the luminance adaptation curve (see the left figure of

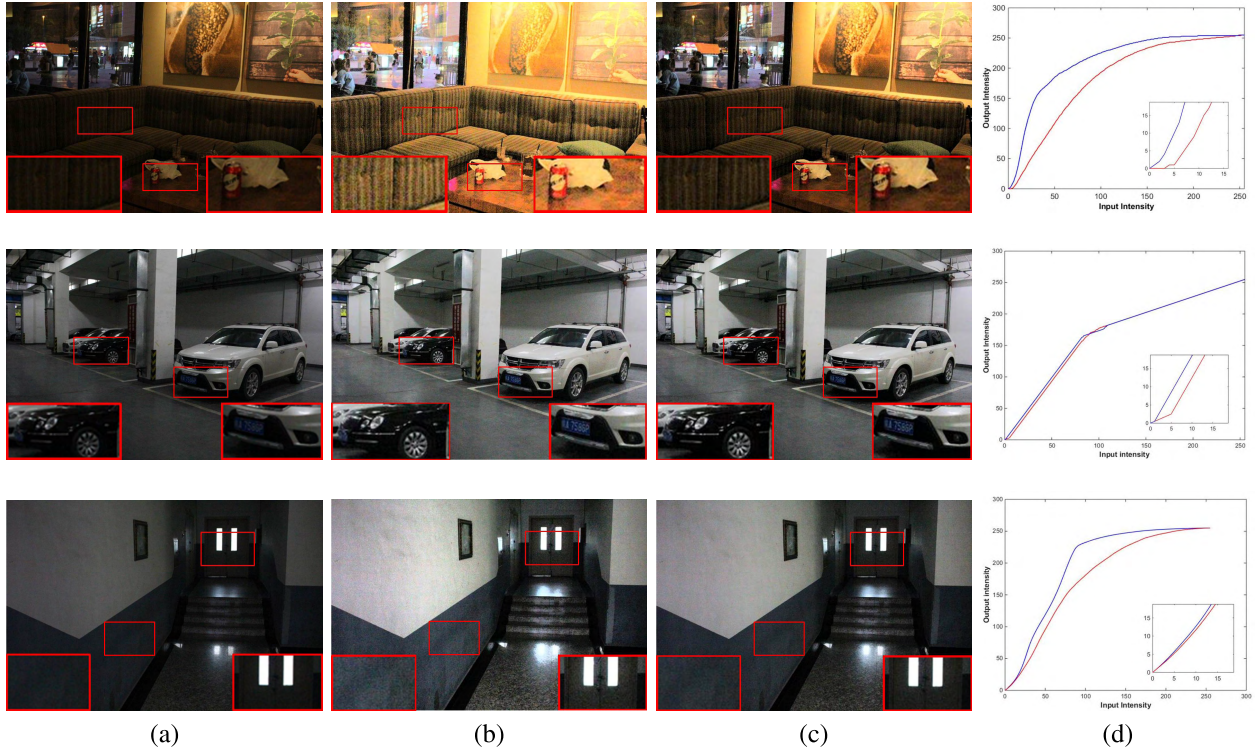


**FIGURE 4.** Contrast enhancement results in *Restaurant*, *Car*, and *Classroom* by HE, OCTM [6] and AGCWD [7]. (a) Original image. (b) Enhancement by the original histogram. (c) Enhancement by the noise aware histogram. (d) Mapping curve by the original histogram (blue) and the noise aware histogram (red). The first row is processed by HE, the second one by OCTM and the third one by AGCWD. The enhanced color images are obtained by Section III-C.

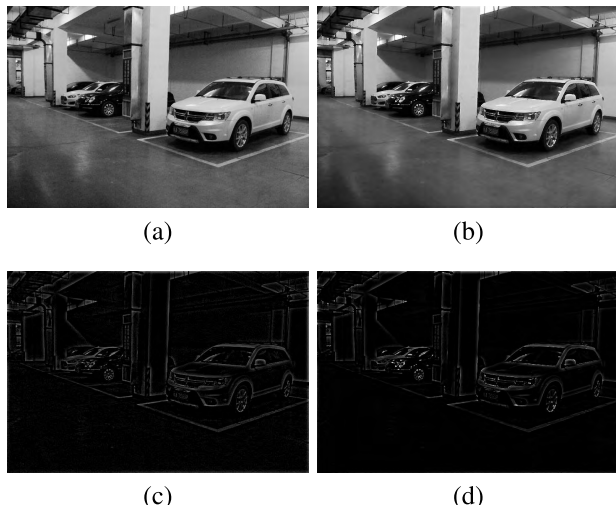


**FIGURE 5.** Perceptual noise reduction for *Car*. (a) Result after noise aware contrast enhancement. (b) Perceptual noise reduction for (a). (c) Detail layer of (a). (d) Perceptual noise reduction of (c).

Fig. 1(b)) [36] as follows:

$$V(l(x, y)) = \begin{cases} k_1 \cdot (1 - \frac{2l(x, y)}{256})^{\lambda_1} + 1 & l(x, y) \leq 128 \\ k_2 \cdot (\frac{2l(x, y)}{256} - 1)^{\lambda_2} + 1 & l(x, y) > 128 \end{cases} \quad (9)$$

where  $k_1$ ,  $k_2$ ,  $\lambda_1$ , and  $\lambda_2$  are constants, i.e. 2.0, 0.8, 3.0, and 2.0, respectively. Fig. 6(a) shows the normalized luminance adaptation map  $LA(x, y)$  for *Car*. Based on  $LA(x, y)$ , the image is divided into three parts: 1) Bright regions (i.e., intensity is larger than 128):  $LA(x, y)$  is larger than 1 (see the white pixels in Fig. 6(b)) because JND thresholds increase with the increase of pixel intensity larger than 128 (see the left figure in Fig. 1(b)); 2) Dark regions (i.e., intensity is between 0 and 15):  $LA(x, y)$  is approximately equal to 1 (see the gray pixels in Fig. 6(b)) because noise aware contrast enhancement suppresses the enhancement degree in dark regions; 3) Low intensity regions (i.e., intensity is between 15 and 127):  $LA(x, y)$  is smaller than 1 (see the black pixels in Fig. 6(b)) because the increase of intensity in the contrast enhancement leads to reduction of JND thresholds (see the left figure in Fig. 1(b)). Moreover, we get the visual masking  $VM(x, y)$  [35] as follows:

$$VM(x, y) = \begin{cases} 1 & LA(x, y) \geq 1 \\ (VM'(x, y) + \alpha)^\beta & LA(x, y) < 1 \end{cases} \quad (10)$$

where

$$VM'(x, y) = \frac{1.84Lc(l'(x, y))^{2.4}}{Lc(l'(x, y))^2 + 26^2} \cdot \frac{0.3N(l'(x, y))^{2.7}}{N(l'(x, y))^2 + 1} \quad (11)$$

where  $\alpha$  and  $\beta$  are constants with 0.5-0.9 and 1.3-2.0 respectively. We first obtain  $VM'(x, y)$  from luminance contrast

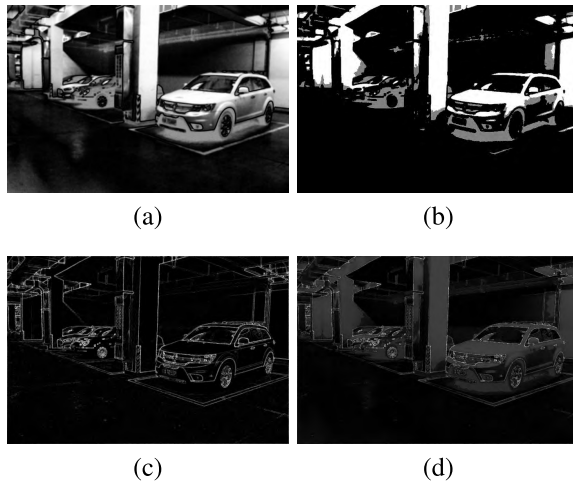


**FIGURE 6.** Two perceptual factors map and their combined noise reduction degree maps. (a) Normalized luminance adaptation factor map  $LA(x, y)$  by (8). (b) Classified regions based on (a) (white pixels:  $LA(x, y) > 1$  in bright regions, gray ones:  $LA(x, y) \approx 1$  in very dark regions, and black ones:  $LA(x, y) < 1$  in low intensity regions). (c) Normalized visual masking factor map  $VM'(x, y)$  by (11) (large intensity represents high visual masking and small one mean low visual masking). (d) Normalized noise reduction degree map by the fusion of two perceptual factors in (8) and (10), i.e.  $VM(x, y) \cdot LA(x, y)$ .

$Lc(x, y)$  and gradient regularity  $N(x, y)$  by (11), and then normalize it by min-max normalization. The normalized  $VM'(x, y)$  is the input for the transfer function (10).  $Lc(x, y)$  and  $N(x, y)$  represent gradient magnitude and gradient regularity in a local region, respectively [35].  $VM'(x, y)$  extracts most of details and textures from the noisy image as shown in Fig. 6(c) because textural regions have higher visual masking effects than smooth ones. High visual masking effects mean that noise is hardly detected by HVS, and thus noise reduction in textural regions can be performed in a small degree. However, noise in smooth regions should be greatly reduced due to the low visual masking effect. Thus, the noise reduction is larger in smooth regions than that in texture regions, which is beneficial to detail preservation in images.  $LA(x, y) < 1$  represents noise reduction in low intensity regions, and we use visual masking to extract textures in noisy images. In (10),  $\alpha$  determines boundary points which divide the mapping curve into two parts:  $VM'(x, y)$  is smaller or greater than  $1 - \alpha$ . The boundary points are located at  $VM'(x, y) = 1 - \alpha$ .  $\beta$  adjusts the slope of the mapping curve. Fig. 7 shows transfer functions according to different  $\alpha$  and  $\beta$ . As shown in Fig. 7(a), large  $VM'(x, y)$  (greater than  $1 - \alpha$ ) in texture regions is mapped beyond 1 to enhance them, while small  $VM'(x, y)$  (smaller than  $1 - \alpha$ ) in smooth regions is mapped below 1 to suppress noise. Larger  $\alpha$  leads to smaller boundary points, which considers weaker details as texture and thus preserves them. As shown in Fig. 7(b),  $\beta$  adjusts the slope of the mapping curve and larger  $\beta$  increases the slope. Since  $LA(x, y) \geq 1$  represents the detail enhancement and preservation in bright and dark regions, visual masking is not considered, i.e.  $VM(x, y) = 1$ . As shown in Fig. 6(d), the noise reduction degree map, i.e. the fusion of two

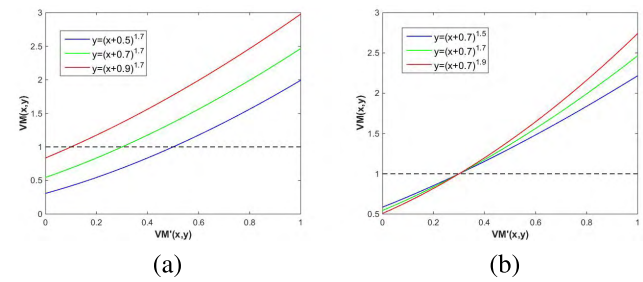


**FIGURE 7.** Mapping curves of  $VM(x, y) = (VM'(x, y) + \alpha)^{\beta}$  in (10). (a) Different  $\alpha$ . (b) Different  $\beta$ .

perceptual factors in (8) and (10),  $VM(x, y) \cdot LA(x, y)$ , for detail layer shows three parts: 1) The detail layer in bright and dark regions is enhanced based on luminance adaptation (see the gray pixels); 2) Edges and textures extracted by visual masking are enhanced in a large degree (see the white pixels); 3) Remained noise in low intensity regions are suppressed (see the black pixels). Figs. 5(b) and (d) show the detail-preserved noise reduction result in *Car*. It is shown that perceptual noise reduction removes noise while preserving most details compared with the noisy image in Figs. 5(a) and (c).

### C. COLOR ENHANCEMENT

Finally, we perform color enhancement by Schlick's method [37] as follows:

$$M_e(x, y) = \left( \frac{M_o(x, y)}{l(x, y)} \right)^{\gamma} \cdot l_e(x, y) \quad (12)$$

where  $M_e(x, y)$  and  $M_o(x, y)$  are trichromatic channel values of the output color and original images, respectively;  $l_e(x, y)$  and  $l(x, y)$  are gray images from the noise reduction result and the original image, respectively; and a correction factor  $\gamma$  is between 0.6 and 1.0. Fig. 8 shows the final enhancement result after color enhancement in (12) and color space conversion ( $YUV \rightarrow RGB$ ). Color enhancement reproduces vivid and saturated colors as shown in Fig. 8(c) compared to the results without color enhancement in Fig. 8(b). We provide their zoomed regions of (a), (b) and (c) in Fig. 8(d).

### III. EXPERIMENTAL RESULTS

For experiments, we use a PC with Intel (R) Core (TM) i5 CPU (2.60GHZ) and 4.00GB RAM running a Windows 7 environment and MATLAB. We use nine test images for tests and divide them into three types: 1) General low light images: *Car*, *Classroom*, *Chair* and *Bookshelf*; 2) Low light images with non uniform lights: *Restaurant* and *Sofa*; 3) Extremely low light images: *Greenwich*, *Ramp* and *Buildings*. *Greenwich* is obtained from *Greenwich* database [38] with the resolution of  $652 \times 916$ , while *Ramp* is from [39] with  $576 \times 720$ . The other images are captured by a digital camera (Canon EOS 60D) with  $480 \times 720$ . They have a dark tone with a narrow dynamic range and much noise. We compare the proposed method with three other methods: content aware dark image enhancement (CADIE) [22], automatic contrast

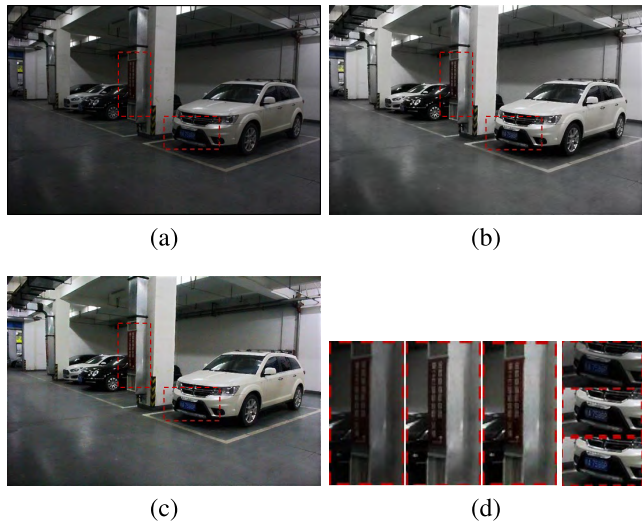


**FIGURE 8.** Color enhancement results in *Car*. (a) Original image. (b) Color space conversion ( $YUV \rightarrow RGB$ ). (c) Color enhancement. (d) Zoomed regions of (a), (b) and (c).

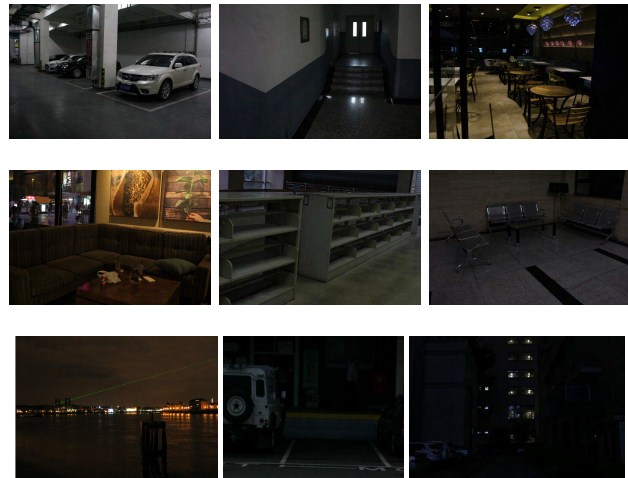


**FIGURE 9.** Test images for experiments. Top left to bottom right: *Car*, *Classroom*, *Restaurant*, *Sofa*, *Bookshelf*, *Chair*, *Greenwich*, *Ramp*, and *Buildings*.

enhancement based on wavelet coefficient (ACEWC) [19], and low light image enhancement with contrast enlarging and denoising (LLIE) [16].

#### A. SUBJECTIVE EVALUATIONS

Twenty persons took part in the subjective experiments and compared the enhancement results by four methods in terms of four aspects [22]:

1) Structural similarity which assesses the structural similarity of the enhancement result considering potential enhancement. Each person chooses the most closest enhancement result in structure compared to the original image;

2) Details which evaluate detail preservation and enhancement from the enhancement results. Each person chooses the best enhancement result in detail preservation comparing with the original image;

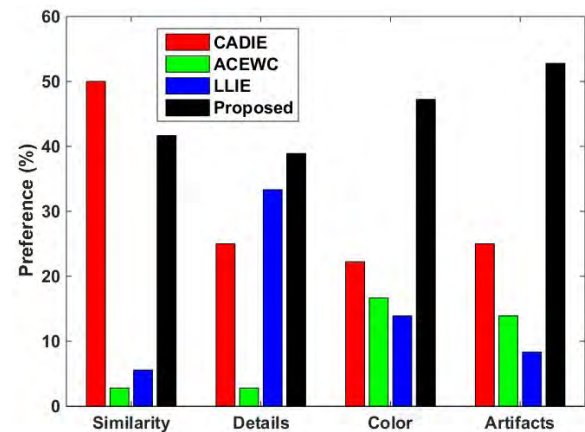


**FIGURE 10.** Preference comparison between different methods in terms of similarity, details, color, and artifacts.

3) Color which refers to color saturation enhancement. Each person selects the best enhancement result in color saturation without the color cast problem;

4) Artifacts which mainly consider noise amplification and over enhancement problem. Each person need to choose the enhancement result with the least visible noise and contrast over stretching.

Fig. 10 shows preference percentages for each method in terms of four aspects. Experimental results show the proposed method achieves the best performance in details, color, and artifacts, while CADIE [22] obtains good performance in structural similarity. Fig. 11 shows experimental results of the proposed methods compared with CADIE [22], ACEWC [19], and LLIE [16]. CADIE [22] conducts content-aware histogram equalization by edge-contrast pairs. However, low dynamic range and severe noise in low light condition degrades image edges and transforms edge-contrast pairs into smooth pairs. Thus, CADIE [22] weakens the degree of contrast enhancement especially for extremely low light images such as *Greenwich*, *Ramp*, and *Buildings* (see the third column of Fig. 11). Thus, CADIE [22] produces relatively dark results which looks similar to the original image in perception compared to other enhancement results as shown in the third column of Fig. 11. In the experiments, CADIE [22] obtains the best performance in structure similarity. However, insufficient enhancement in luminance and contrast leads to the limited detail enhancement, and thus meaningful details and contrast are lost in the results. ACEWC [19] achieves good contrast improvement but produces too much noise and over-stretches contrast in the results such as wall in *Car* and ground in *Classroom* in the second column of Fig. 11. The main reason is that the contrast enhancement in ACEWC [19] is done by CLAHE [4] which does not consider the noise level (see the left figure in Fig. 1(a)) and image locality. CLAHE produces serious over enhancement in dark and smooth regions such as the red box in the second column of Fig. 11. Thus, ACEWC [19] obtains the lower score in structural similarity and details by subjective evaluations.

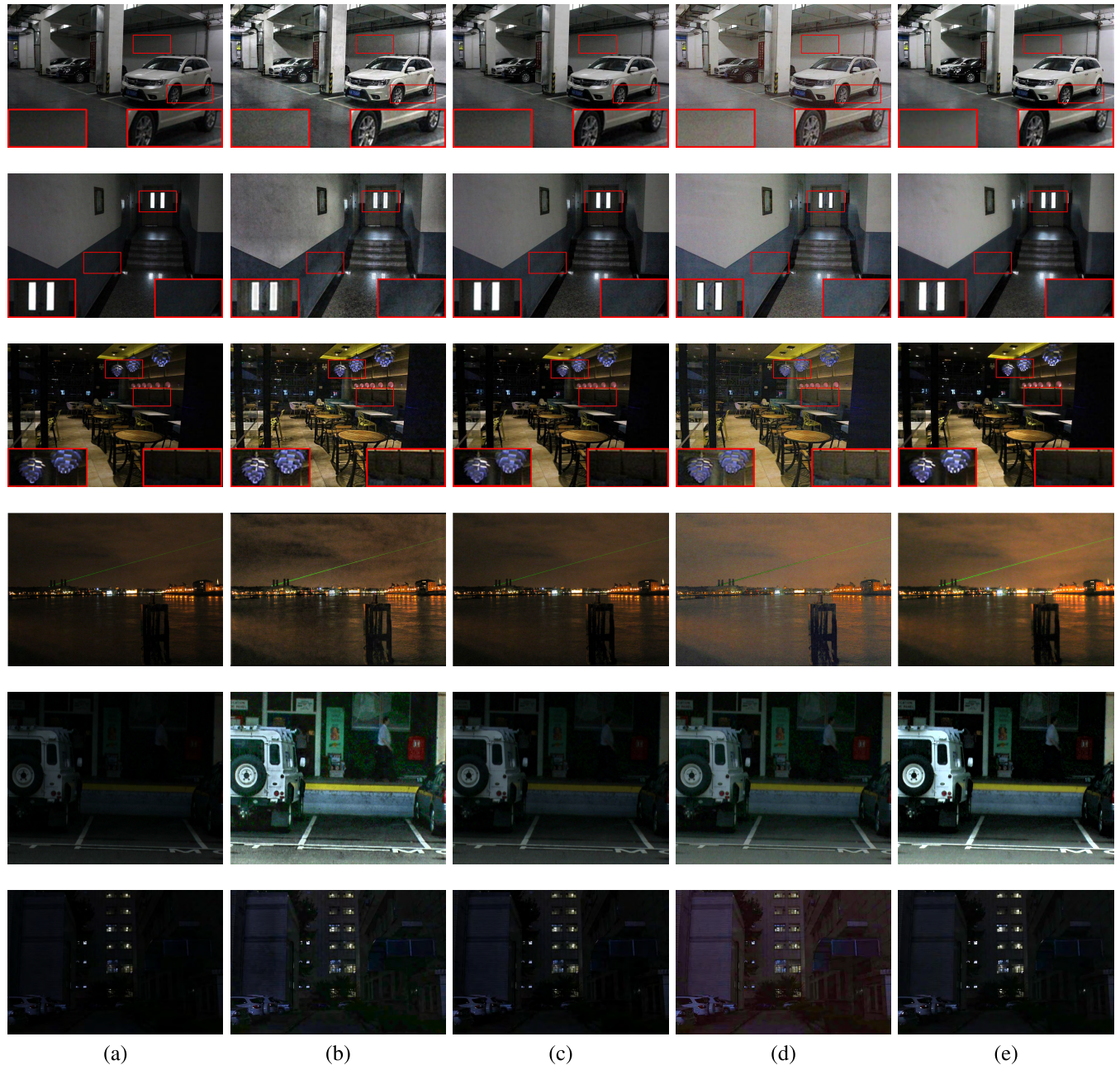


**FIGURE 11.** Experimental results for three test images. Top to bottom: **Car**, **Classroom**, **Restaurant**, **Greenwich**, **Ramp**, and **Buildings**. (a) Original images. (b) ACEWC [19]. (c) CADIE [22]. (d) LLIE [16]. (e) Proposed method.

LLIE [16] provides the strongest luminance enhancement with more visible details in the whole images by dehazing-based contrast enhancement. Therefore, LLIE [16] achieves better performance in details. However, noise is also enhanced and distributed in the whole image, especially in dark regions (see the fourth column of Fig. 11). LLIE [16] also introduces the color cast problem and serious color noise in *Car* and *Buildings*, and thus obtains the worst performance in artifacts and color. The proposed method utilizes noise distribution to extract high contrast pixels which has the local contrast larger than relative noise level (RNL), and enhances low light images based on these pixels. Noise aware

contrast enhancement enhances images with noise suppression as shown in Fig. 4. Moreover, perceptual noise reduction suppresses visible noise based on the variation of JND thresholds after contrast enhancement. Also, we use visual masking to extract details and edges from noisy images. That is, we generate different reduction degrees for details and noisy regions based on the visual masking factor. The perceptual noise reduction reduces noise while preserving details in an image. Red boxes in Fig. 11 show that the proposed method achieves the least noise amplification among four methods. Furthermore, color enhancement reproduces more saturated colors, which makes the results look more vivid. Above all,

**TABLE 1.** Performance comparison between CADIE [22], ACEWC [19], LLIE [16] and proposed method.

Metrics	Methods	Car	Classroom	Restaurant	Sofa	Bookshelf	Chair	Greenwich	Ramp	Buildings	Average
Luminance	Original	1.0000	1.0000	1.0000	1.0000	1.0000	1.0000	1.0000	1.0000	1.0000	1.0000
	CADIE [22]	1.3406	1.4043	1.2974	1.2260	1.4227	1.5949	1.3470	1.8552	1.6407	1.4588
	ACEWC [19]	1.7174	1.7451	1.7373	1.6362	1.8903	1.4400	1.7395	<b>6.1440</b>	3.0189	2.3410
	LLIE [16]	<b>2.1189</b>	<b>2.3288</b>	<b>2.2446</b>	<b>1.9993</b>	<b>2.2149</b>	<b>2.6935</b>	<b>2.8856</b>	3.4181	<b>4.8186</b>	<b>2.7469</b>
	Proposed	1.7133	1.8186	1.4988	1.6321	1.8778	1.9621	2.3188	4.7067	2.8310	2.2621
Contrast	Original	1.0000	1.0000	1.0000	1.0000	1.0000	1.0000	1.0000	1.0000	1.0000	1.0000
	CADIE [22]	1.1591	1.2063	1.2623	1.0475	1.3338	1.7458	1.0834	1.7510	1.3650	1.3282
	ACEWC [19]	1.4565	1.2694	1.2839	1.1443	1.8674	1.4078	1.1547	4.3316	1.6044	1.7244
	LLIE [16]	1.0507	1.4155	1.3679	0.9442	1.5619	<b>2.0894</b>	1.1229	2.6326	1.6660	1.5390
	Proposed	<b>1.4597</b>	<b>1.7279</b>	<b>1.4954</b>	<b>1.4794</b>	<b>1.9100</b>	1.8980	<b>1.8395</b>	<b>4.9411</b>	<b>1.8500</b>	<b>2.0657</b>
Structure	Original	1.0000	1.0000	1.0000	1.0000	1.0000	1.0000	1.0000	1.0000	1.0000	1.0000
	CADIE [22]	<b>0.9877</b>	<b>0.9805</b>	<b>0.9926</b>	<b>0.9892</b>	<b>0.9843</b>	<b>0.9759</b>	<b>0.9873</b>	<b>0.9988</b>	<b>0.9598</b>	<b>0.9840</b>
	ACEWC [19]	0.9319	0.9131	0.9399	0.8806	0.9293	0.9132	0.8088	0.9454	0.9208	0.9092
	LLIE [16]	0.8979	0.9249	0.9505	0.9296	0.9456	0.9339	0.7724	0.9703	0.8041	0.9032
	Proposed	0.9585	0.9556	<b>0.9914</b>	0.9636	<b>0.9857</b>	<b>0.9719</b>	0.8818	<b>0.9899</b>	0.9258	0.9582
DE	Original	6.8507	6.1156	5.9414	6.6693	6.5209	5.7307	5.6266	4.7971	3.9553	5.8008
	CADIE [22]	7.2266	6.5853	6.1575	7.0432	6.8698	6.5574	5.9844	5.1580	4.7753	6.2619
	ACEWC [19]	<b>7.5622</b>	<b>6.9628</b>	<b>6.8259</b>	7.2648	<b>7.4683</b>	6.3046	6.3600	<b>7.3037</b>	5.1944	<b>6.8052</b>
	LLIE [16]	7.2134	6.8829	6.9409	7.1992	7.0589	6.6256	6.3634	6.4785	<b>5.7023</b>	6.7183
	Proposed	<b>7.5204</b>	<b>6.9086</b>	6.4228	<b>7.3326</b>	<b>7.4184</b>	<b>6.6364</b>	<b>6.8958</b>	6.7107	5.3249	<b>6.7967</b>
Color	Original	0.1445	0.1275	0.4080	0.6103	0.1656	0.1088	0.3914	0.0905	0.0064	0.2281
	CADIE [22]	0.1318	0.1511	0.4773	0.6328	0.1774	0.1332	0.4355	0.2121	0.0487	0.2667
	ACEWC [19]	0.2262	0.2170	0.5315	0.6653	0.2645	0.1186	0.5156	<b>0.6554</b>	0.1967	0.3768
	LLIE [16]	<b>0.2330</b>	<b>0.3245</b>	<b>0.5945</b>	0.6307	<b>0.3486</b>	<b>0.2801</b>	0.5499	0.3880	<b>0.2503</b>	<b>0.4000</b>
	Proposed	0.2190	0.2108	0.5286	<b>0.7837</b>	0.2638	0.1877	<b>0.6300</b>	0.4948	0.1709	0.3877

Bold numbers represent the best or equally best performance in each metric.

the proposed method enhances low light images with the minimum noise amplification while successfully preserving details as shown in the fifth column of Fig. 11.

## B. QUANTITATIVE EVALUATIONS

For quantitative measurements, we evaluate the performance in terms of five quantitative measures. Three measures are luminance index  $l$ , contrast index  $c$ , and structural index  $s$ , and calculated as follows [22]:

$$l(l_e, l) = \frac{\mu_{l_e}}{\mu_l} \quad (13)$$

$$c(l_e, l) = \frac{\sigma_{l_e}}{\sigma_l} \quad (14)$$

$$s(l_e, l) = \frac{\sigma_{l_e, l} + k}{\sigma_{l_e} \sigma_l + k} \quad (15)$$

where  $l_e$  and  $l$  are gray images from the noise reduction result and the original image in (12), respectively;  $\mu_l$  is the mean intensity in an image  $l$ ;  $\sigma_l$  is the standard deviation of  $l$ ; and  $\sigma_{l_e, l}$  is covariance between  $l_e$  and  $l$ . Three measures evaluate luminance enhancement, contrast enhancement, and structural similarity between the original images and their enhanced results, respectively. The other two measures are discrete entropy (DE) [40] and colorfulness [41] which are estimated by:

$$H(p) = - \sum_{i=0}^{L-1} p(i) \log_2 p(i) \quad (16)$$

$$cl(M) = 0.02 \times \log\left(\frac{\sigma_\alpha^2}{|\mu_\alpha|^{0.2}}\right) \times \log\left(\frac{\sigma_\beta^2}{|\mu_\beta|^{0.2}}\right) \quad (17)$$

where  $p$  is the probability density function and  $L$  is total intensity levels, i.e. 256;  $M$  is the trichromatic channel value in (12) which contains three channels, i.e. R, G and B in color images;  $\alpha = R - G$  and  $\beta = 0.5(R + G) - B$  are opponent red-green and yellow-blue spaces;  $\sigma_\alpha^2$ ,  $\sigma_\beta^2$ ,  $\mu_\alpha$  and  $\mu_\beta$  are variance and mean values in  $\alpha$  and  $\beta$ . DE represents the amount of information in an image. Colorfulness measures color chrominance attributes from the enhanced results by human perception. Table 1 shows evaluation results of four methods on nine test images in terms of the five measures. High values in luminance and contrast mean strong luminance and contrast enhancement. Structural index is closer to 1.0, which means the enhanced results are more similar to their original images in structure. Higher DE means more details, while larger colorfulness metric represents more saturated colors in an image. For luminance index, LLIE [16] obtains the brightest images but produces the lower contrast in the enhanced results because dehazing-based contrast enhancement provides the strongest luminance enhancement in the whole images including dark regions. Thus, the results by LLIE [16] looks foggy and suffers from severe noise amplification in dark regions as shown in the fourth column of Fig. 11. In contrast, noise aware contrast enhancement suppresses enhancement in dark regions and provides large enhancement in high contrast regions. Thus, the proposed method achieves the best performance in local contrast, which produces good contrast as shown in the fifth column of Fig. 11. In structural similarity, CADIE [22] obtains the closest enhanced results to the original images, which is mentioned in subjective evaluations. However, the proposed method acquires the second best performance in structural similarity with better enhancement in luminance and contrast

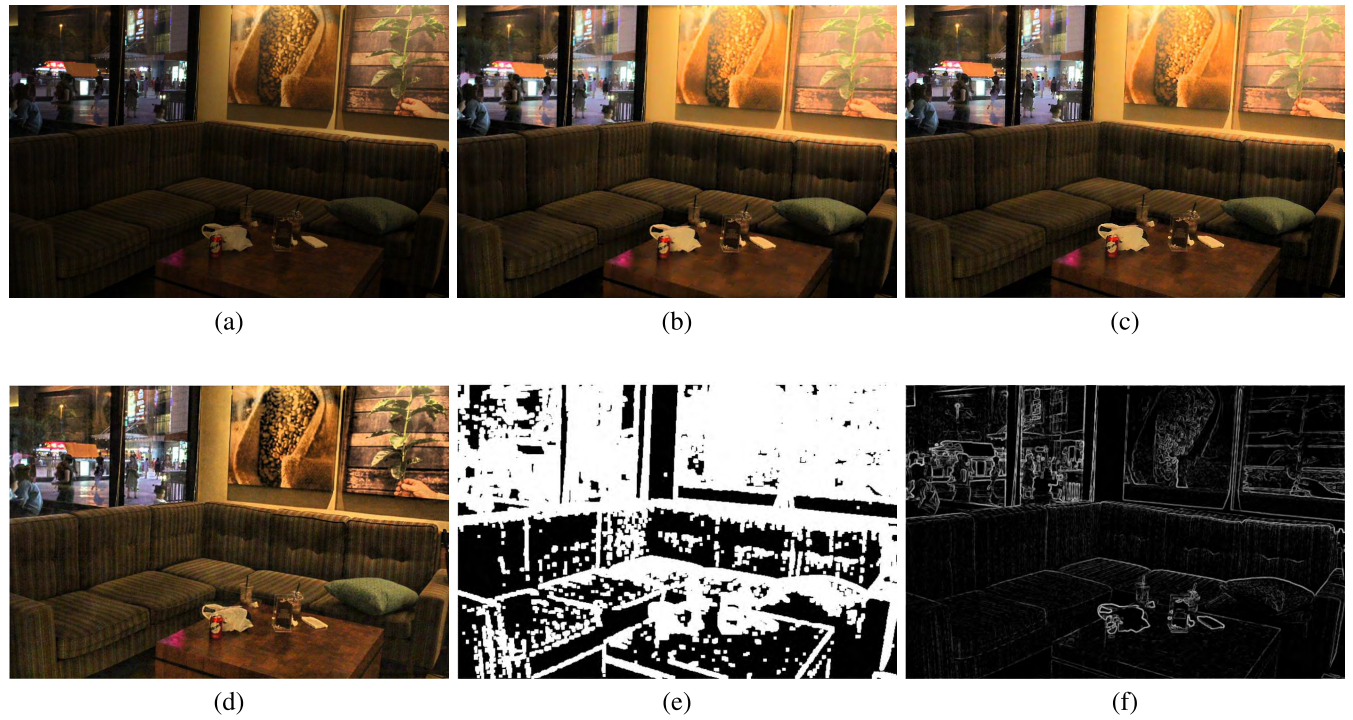


**FIGURE 12.** Experimental results by [1], the proposed method, and [21]. (a) Original image. (b) [1]. (c) Proposed method. (d) [21]. (e) Texture map in [1]. (f) Texture map of the proposed method.

compared with CADIE [22] (see the bold numbers in the structure metric of Table 1). Better performance in structure also indicates the proposed method does not generate too much noise amplification and contrast over stretching. In DE, ACEWC [19] and the proposed method achieve equally good performance but ACEWC [19] suffers from noise amplification as shown in the second column of Fig. 11. Thus, ACEWC does not produce good results in details of subjective evaluation. In colorfulness, LLIE [16] and the proposed method produces the best and second results in the saturated colors. In (12), high luminance enhancement leads to over-enhancement in color channels, resulting in large  $cl$ . However, the proposed method does not provide much luminance enhancement due to the noise aware contrast enhancement considering noise characteristics and image locality. Thus, the proposed method looks darker with less colorfulness than LLIE (see *Classroom* and *Restaurant* in Figs. 11(d) and (e)). However, LLIE produces the enhanced result with amplified color noise and thus increases  $cl$  (see *Car* and *Building* in Figs. 11(d) and (e)). Thus, the proposed method achieves the best performance in colors, which is same as subjective evaluations. Therefore, the proposed method achieves the best performance in contrast enhancement while providing good results in structural similarity, detail enhancement, and color enhancement among four methods.

### C. COMPARISON WITH OUR PREVIOUS WORKS

We compared the results of the proposed method with those of our previous works such as [1] (ICASSP 2017)

and [21] (JVCIR 2017). Fig. 12 shows experimental results by three methods. The proposed method and [1] adopt two-step noise suppression for low light image enhancement, and are different in the second step of perceptual noise reduction. Reference [1] estimates texture maps based on the statistical property of textureness [32] with rough region segmentation, while the proposed method extracts texture pixels in an image based on luminance contrast and visual regularity. Thus, the proposed method achieves a more accurate texture map as shown in Figs. 12(e) and (f), and preserves textures better than [1] as shown in Figs. 12(b) and (c) (sofa area). Reference [21] provides the contrast enhancement based on histogram without considering noise characteristics and content in the low pass sub-band. Thus, [21] causes over-enhancement in dark regions with severe noise amplification such as sofa area as shown in Fig. 12(d).

### D. COMPARISON WITH OTHER JND MODELS

In general, JND models are composed of two main categories: luminance adaptation and visual masking. Luminance adaptation shows the variation of visibility threshold according to the change of background luminance, while visual masking represents the visibility reduction of a visual component according to the change of the background. In the proposed method, we use luminance adaptation to measure the noise visibility after contrast enhancement, and visual masking to measure the noise visibility at the presence of the background with different local textures (e.g. smooth and texture regions). Through experiments, we analyze the effects of different JND

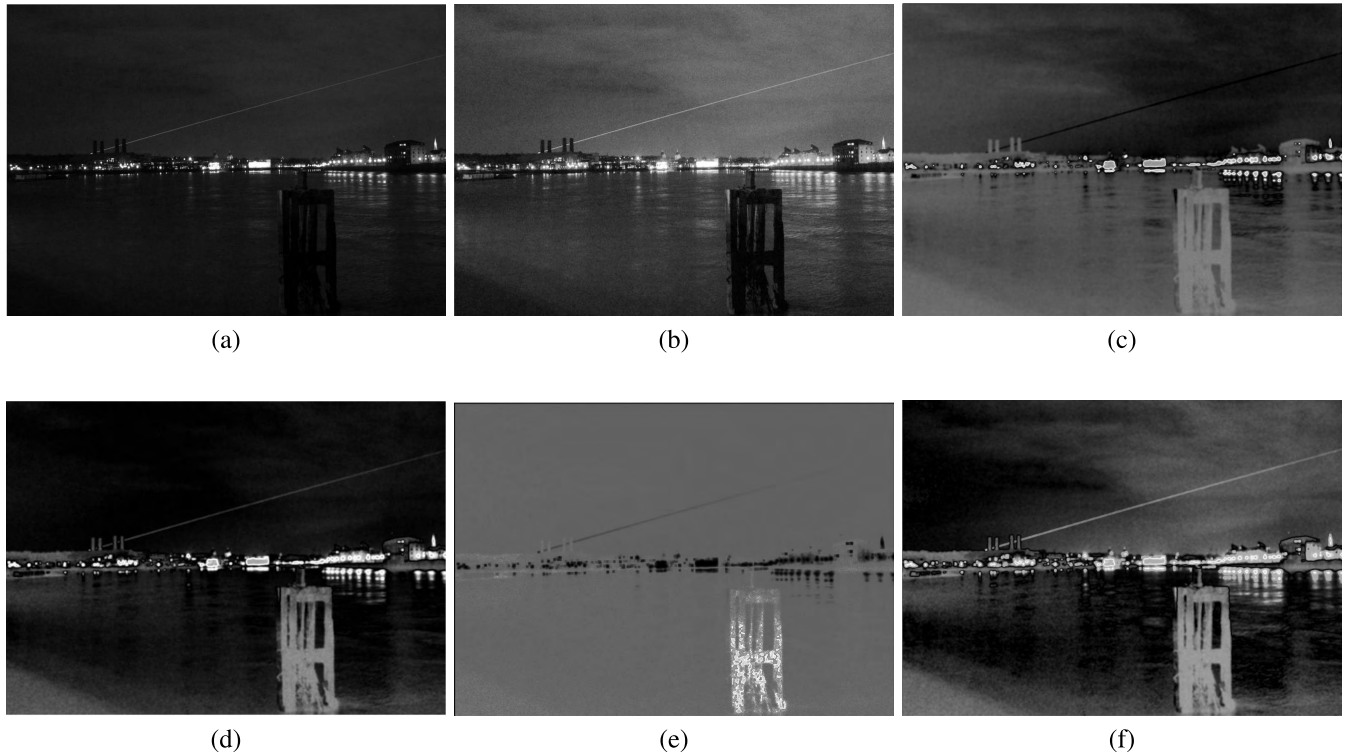


**FIGURE 13.** Luminance adaptation map  $LA(x, y)$ . (a) Original image (gray level). (b) Enhanced result by noise aware contrast enhancement. (c) Eq. (18) [43]. (d) Eq. (9) [36]. (e) Eq. (19) [44]. (f) Eq. (20) [45].

models on the noise visibility in the enhanced results as follows:

### 1) LUMINANCE ADAPTATION MODELS

We obtain four luminance adaptation models in [42] to evaluate the noise visibility change after contrast enhancement as follows:

Model I: [43]

$$V(l(x, y)) = \begin{cases} 17 \cdot (1 - \sqrt{\frac{l(x, y)}{127}}) + 3 & l(x, y) \leq 127 \\ \frac{3}{128} \cdot (l(x, y) - 127) + 3 & l(x, y) > 127 \end{cases} \quad (18)$$

Model II: Eq. (9) [36];

Model III: [44]

$$V(l(x, y)) = \left( \frac{l(x, y)}{128} \right)^{0.649} \quad (19)$$

Model IV: [45]

$$V(l(x, y)) = \begin{cases} (60 - l(x, y))/150 + 1 & l(x, y) \leq 60 \\ 1 & 60 < l(x, y) < 170 \\ (l(x, y) - 170)/425 + 1 & l(x, y) \geq 170 \end{cases} \quad (20)$$

Fig. 13 shows  $LA(x, y)$  by four luminance adaptation models. Compared to Models I and III [43], [44], Model II [36] shows the most luminance variation in water

area between the original image in Fig. 13(a) and its enhanced result in Fig. 13(b), and achieves different noise reduction degrees according to regions. Model II also leads to less noise amplification as shown in Figs. 13 (d) and (f) compared to Model IV [45]. Thus, we select Model II [36] to estimate the visibility threshold and reduce noise caused by contrast enhancement.

### 2) VISUAL MASKING MODELS

Visual masking considers contrast masking, pattern masking, and both of them. Reference [46] estimates the contrast masking using edge detection to improve the JND estimation in edge and non-edge regions. Reference [47] introduces the structure uncertainty into pattern masking because HVS has the different sensitivity to visual regularity. References [35] and [48] improve pattern masking by content regularity, i.e. gradient regularity. Reference [48] provides a visual masking model considering both contrast masking and pattern masking, while [35] provides easy computation. We use three visual masking models of [35], [46], and [47] for performance comparison. Fig. 14 shows visual masking maps by three visual masking models. As shown in Fig. 14 (d), [35] extracts main textures in the enhanced result while suppressing weak details, which leads to enhancement of main details without amplification of weak details in the noise reduction step. This is because noise and weak details are easily fused in an image. Reference [46] captures weak textures and noise in the visual masking map



**FIGURE 14.** Visual masking. (a) Noise aware contrast enhancement result. Three visual masking maps by (b) [46], (c) [47], and (d) [35].

as shown in Fig. 14(b), which leads to the enhancement of both details and noise in the noise reduction step. The visual masking map (Fig. 14(c)) by [47] seems to be blurry and cannot represent accurate textures such as paintings on the wall. Thus, we use [35] to estimate visual masking in the proposed method, thus resulting in outstanding detail enhancement.

#### IV. CONCLUSIONS

In this paper, we have proposed perceptual enhancement of low light images based on two-step noise suppression. Contrast enhancement increases the intensity in images while decreasing the visibility threshold, which makes noise much visible. Thus, we have employed two-step noise reduction to deal with this problem. First, we have performed noise aware contrast enhancement based on noise characteristics and image locality to prevent noise amplification after contrast enhancement. Second, we have perceptually reduced noise in images while preserving details using a JND model which represents noise visibility in contrast enhancement. Experiment results demonstrate that the proposed method successfully enhances contrast and colors in low light images while minimizing noise amplification and preserving most details.

#### REFERENCES

- [1] H. Su and C. Jung, "Low light image enhancement based on two-step noise suppression," in *Proc. IEEE Int. Conf. Acoust., Speech, Signal Process. (ICASSP)*, Mar. 2017, pp. 1977–1981.
- [2] E. P. Bennett and L. McMillan, "Video enhancement using per-pixel virtual exposures," *ACM Trans. Graph.*, vol. 24, no. 3, pp. 845–852, 2005.
- [3] Q. Xu, H. Jiang, R. Scopigno, and M. Sbert, "A novel approach for enhancing very dark image sequences," *Signal Process.*, vol. 103, pp. 309–330, Oct. 2014.
- [4] E. D. Pisano *et al.*, "Contrast limited adaptive histogram equalization image processing to improve the detection of simulated speculations in dense mammograms," *J. Digit. Imag.*, vol. 11, no. 4, pp. 193–200, 1998.
- [5] T. Arici, S. Dikbas, and Y. Altunbasak, "A histogram modification framework and its application for image contrast enhancement," *IEEE Trans. Image Process.*, vol. 18, no. 9, pp. 1921–1935, Sep. 2009.
- [6] X. Wu, "A linear programming approach for optimal contrast-tone mapping," *IEEE Trans. Image Process.*, vol. 20, no. 5, pp. 1262–1272, May 2011.
- [7] S.-C. Huang, F.-C. Cheng, and Y.-S. Chiu, "Efficient contrast enhancement using adaptive gamma correction with weighting distribution," *IEEE Trans. Image Process.*, vol. 22, no. 3, pp. 1032–1041, Mar. 2013.
- [8] Z. Ling, Y. Liang, Y. Wang, H. Shen, and X. Lu, "Adaptive extended piecewise histogram equalisation for dark image enhancement," *IET Image Process.*, vol. 9, no. 11, pp. 1012–1019, 2015.
- [9] D. J. Jobson, Z.-U. Rahman, and G. A. Woodell, "A multiscale Retinex for bridging the gap between color images and the human observation of scenes," *IEEE Trans. Image Process.*, vol. 6, no. 7, pp. 965–976, Jul. 1997.
- [10] S. S. Agaian, B. Silver, and K. A. Panetta, "Transform coefficient histogram-based image enhancement algorithms using contrast entropy," *IEEE Trans. Image Process.*, vol. 16, no. 3, pp. 741–758, Mar. 2007.
- [11] J. Mukherjee and S. K. Mitra, "Enhancement of color images by scaling the DCT coefficients," *IEEE Trans. Image Process.*, vol. 17, no. 10, pp. 1783–1794, Oct. 2008.
- [12] A. Halimi, G. S. Buller, S. McLaughlin, and P. Honeine, "Denoising smooth signals using a Bayesian approach: Application to altimetry," *IEEE J. Sel. Topics Appl. Earth Observ. Remote Sens.*, vol. 10, no. 4, pp. 1278–1289, Apr. 2017.
- [13] H.-M. Hu, Y. Gao, Q. Guo, and B. Li, "A region-based video de-noising algorithm based on temporal and spatial correlations," *Neurocomputing*, vol. 266, pp. 361–374, Nov. 2017.
- [14] Y. Zheng, H. Cui, C. Wang, and J. Zhou, "Privacy-preserving image denoising from external cloud databases," *IEEE Trans. Inf. Forensics Security*, vol. 12, no. 6, pp. 1285–1298, Jun. 2017.
- [15] X. Dong *et al.*, "Fast efficient algorithm for enhancement of low lighting video," in *Proc. IEEE Int. Conf. Multimedia Expo.*, Jul. 2011, pp. 1–6.
- [16] L. Li, R. Wang, W. Wang, and W. Gao, "A low-light image enhancement method for both denoising and contrast enlarging," in *Proc. IEEE Int. Conf. Image Process. (ICIP)*, Sep. 2015, pp. 3730–3734.
- [17] X. Zhang, P. Shen, L. Luo, L. Zhang, and J. Song, "Enhancement and noise reduction of very low light level images," in *Proc. Int. Conf. Pattern Recognit. (ICPR)*, Nov. 2012, pp. 2034–2037.
- [18] W. Shi, C. Chen, F. Jiang, D. Zhao, and W. Shen, "Group-based sparse representation for low lighting image enhancement," in *Proc. IEEE Int. Conf. Image Process. (ICIP)*, Sep. 2016, pp. 4082–4086.
- [19] A. Loza, D. R. Bull, P. R. Hill, and A. M. Achim, "Automatic contrast enhancement of low-light images based on local statistics of wavelet coefficients," *Digit. Signal Process.*, vol. 23, no. 6, pp. 1856–1866, 2013.
- [20] T. Sun and C. Jung, "Readability enhancement of low light images based on dual-tree complex wavelet transform," in *Proc. IEEE Int. Conf. Acoust., Speech, Signal Process. (ICASSP)*, Mar. 2016, pp. 1741–1745.
- [21] C. Jung, Q. Yang, T. Sun, Q. Fu, and H. Song, "Low light image enhancement with dual-tree complex wavelet transform," *J. Vis. Communun. Image Represent.*, vol. 42, pp. 28–36, Jan. 2017.
- [22] A. R. Rivera, B. Ryu, and O. Chae, "Content-aware dark image enhancement through channel division," *IEEE Trans. Image Process.*, vol. 21, no. 9, pp. 3967–3980, Sep. 2012.
- [23] J. Lim, J.-H. Kim, J.-Y. Sim, and C.-S. Kim, "Robust contrast enhancement of noisy low-light images: Denoising-enhancement-completion," in *Proc. IEEE Int. Conf. Image Process. (ICIP)*, Sep. 2015, pp. 4131–4135.
- [24] X. Liu, G. Cheung, and X. Wu, "Joint denoising and contrast enhancement of images using graph laplacian operator," in *Proc. IEEE Int. Conf. Acoust., Speech, Signal Process. (ICASSP)*, Apr. 2015, pp. 2274–2278.
- [25] R. Chouhan, R. K. Jha, and P. K. Biswas, "Enhancement of dark and low-contrast images using dynamic stochastic resonance," *IET Image Process.*, vol. 7, no. 2, pp. 174–184, Mar. 2013.
- [26] R. K. Jha, R. Chouhan, P. K. Biswas, and K. Aizawa, "Internal noise-induced contrast enhancement of dark images," in *Proc. 19th IEEE Int. Conf. Image Process. (ICIP)*, Sep. 2012, pp. 973–976.
- [27] D. Sugimura, T. Mikami, H. Yamashita, and T. Hamamoto, "Enhancing color images of extremely low light scenes based on RGB/NIR images acquisition with different exposure times," *IEEE Trans. Image Process.*, vol. 24, no. 11, pp. 3586–3597, Nov. 2015.

- [28] H. Malm, M. Oskarsson, E. Warrant, P. Clarberg, J. Hasselgren, and C. Lejdfor, "Adaptive enhancement and noise reduction in very low light-level video," in *Proc. IEEE 11th Int. Conf. Comput. Vis.*, Oct. 2007, pp. 1–8.
- [29] M. Kim, D. Park, D. K. Han, and H. Ko, "A novel approach for denoising and enhancement of extremely low-light video," *IEEE Trans. Consum. Electron.*, vol. 61, no. 1, pp. 72–80, Feb. 2015.
- [30] S. M. Pizer *et al.*, "Adaptive histogram equalization and its variations," *Comput. Vis., Graph., Image Process.*, vol. 39, no. 3, pp. 355–368, 1987.
- [31] A. Foi, M. Trimeche, V. Katkovnik, and K. Egiazarian, "Practical Poissonian-Gaussian noise modeling and fitting for single-image raw-data," *IEEE Trans. Image Process.*, vol. 17, no. 10, pp. 1737–1754, Oct. 2008.
- [32] X. Liu, M. Tanaka, and M. Okutomi, "Practical signal-dependent noise parameter estimation from a single noisy image," *IEEE Trans. Image Process.*, vol. 23, no. 10, pp. 4361–4371, Oct. 2014.
- [33] P. Chatterjee, N. Joshi, S. B. Kang, and Y. Matsushita, "Noise suppression in low-light images through joint denoising and demosaicing," in *Proc. IEEE Int. Conf. Comput. Vis. Pattern Recognit. (CVPR)*, Jun. 2011, pp. 321–328.
- [34] G. Eilertsen, R. K. Mantiuk, and J. Unger, "Real-time noise-aware tone mapping," *ACM Trans. Graph.*, vol. 34, no. 6, p. 198, 2015.
- [35] J. Wu, G. Shi, W. Lin, and C. J. Kuo, "Enhanced just noticeable difference model with visual regularity consideration," in *Proc. IEEE Int. Conf. Acoust., Speech Signal Process. (ICASSP)*, Mar. 2016, pp. 1581–1585.
- [36] X. H. Zhang, W. S. Lin, and P. Xue, "Improved estimation for just-noticeable visual distortion," *Signal Process.*, vol. 85, no. 4, pp. 795–808, 2005.
- [37] C. Schlick, "A customizable reflectance model for everyday rendering," in *Proc. 4th Eurograph. Workshop Rendering*, Paris, France, 1993, pp. 73–83.
- [38] A. Dulyan. (2009). *Shutter Speed in Greenwich*. [Online]. Available: [http://commons.wikimedia.org/wiki/File:Shutter\\_speed\\_in\\_Greenwich\\_\(no\\_caption\).jpg](http://commons.wikimedia.org/wiki/File:Shutter_speed_in_Greenwich_(no_caption).jpg)
- [39] (Nov. 2006). *The Eden Project Multi-Sensor Data Set*. [Online]. Available: <http://www.imagefusion.org/>
- [40] C. E. Shannon, *A Mathematical Theory of Communication*. New York, NY, USA: McGraw-Hill, 1974.
- [41] K. Panetta, C. Gao, and S. Agaian, "No reference color image contrast and quality measures," *IEEE Trans. Consum. Electron.*, vol. 59, no. 3, pp. 643–651, Aug. 2013.
- [42] P. Hill, M. E. Al-Mualla, and D. Bull, "Perceptual image fusion using wavelets," *IEEE Trans. Image Process.*, vol. 26, no. 3, pp. 1076–1088, Mar. 2017.
- [43] C.-H. Chou and Y.-C. Li, "A perceptually tuned subband image coder based on the measure of just-noticeable-distortion profile," *IEEE Trans. Circuits Syst. Video Technol.*, vol. 5, no. 6, pp. 467–476, Dec. 1995.
- [44] Z. Liu, L. J. Karam, and A. B. Watson, "JPEG2000 encoding with perceptual distortion control," *IEEE Trans. Image Process.*, vol. 15, no. 7, pp. 1763–1778, Jul. 2006.
- [45] Z. Wei and K. N. Ngan, "Spatio-temporal just noticeable distortion profile for grey scale image/video in DCT domain," *IEEE Trans. Circuits Syst. Video Technol.*, vol. 19, no. 3, pp. 337–346, Mar. 2009.
- [46] X. K. Yang, W. S. Ling, Z. K. Lu, E. P. Ong, and S. S. Yao, "Just noticeable distortion model and its applications in video coding," *Signal Process., Image Commun.*, vol. 20, no. 7, pp. 662–680, Aug. 2005.
- [47] J. Wu, W. Lin, G. Shi, X. Wang, and F. Li, "Pattern masking estimation in image with structural uncertainty," *IEEE Trans. Image Process.*, vol. 22, no. 12, pp. 4892–4904, Dec. 2013.
- [48] J. Wu, L. Li, W. Dong, G. Shi, W. Lin, and C.-C. J. Kuo, "Enhanced just noticeable difference model for images with pattern complexity," *IEEE Trans. Image Process.*, vol. 26, no. 6, pp. 2682–2693, Jun. 2017.



**HAONAN SU** received the B.S. degree in electronic engineering from Xidian University, China, in 2013, where he is currently pursuing the Ph.D. degree. His research interests include image processing and computational photography.



**CHEOLKON JUNG** (M'08) received the B.S., M.S., and Ph.D. degrees in electronic engineering from Sungkyunkwan University, South Korea, in 1995, 1997, and 2002, respectively. He was with the Samsung Advanced Institute of Technology, Samsung Electronics, South Korea, as a Research Staff Member from 2002 to 2007. He was a Research Professor with the School of Information and Communication Engineering, Sungkyunkwan University, from 2007 to 2009. Since 2009, he has been a Professor with the School of Electronic Engineering, Xidian University, China. His main research interests include computer vision, pattern recognition, machine learning, image and video processing, multimedia content analysis and management, computational photography, video coding, and 3-DTV.